Reconfigurable Few-Mode Fiber-Based Microwave Photonic Filter

Elham Nazemosadat and Ivana Gasulla , *Senior Member, IEEE*

Abstract—We experimentally demonstrate, for the first-time to our knowledge, tunable true-time delay line operation over a few-mode fiber link, in which the time delay can be continuously and widely tuned, from 46.3 to 105.6 ps, by simply sweeping the operating optical wavelength over the 35-nm range of the C-band. This has become possible thanks to the particular modal dispersion properties of the developed double-clad step-index few-mode fiber, as it features relatively evenly-spaced incremental chromatic dispersion values among 5 spatial modes. To date, it is the first time a dispersion-diversity FMF with this property has been experimentally reported. We assess the performance of this true-time delay line when applied to microwave signal filtering in both space and wavelength diversities, where a variety of reconfigurable 5, 7 and 10-tap microwave filters with free spectral ranges ranging from 7.7 to 27.1 GHz are experimentally demonstrated.

Index Terms—Few-mode fibers, microwave photonics, microwave filters, space division multiplexing.

I. INTRODUCTION

SPACE-DIVISION multiplexing (SDM) primarily emerged as a promising solution to overcome the capacity limit of conventional single-mode fiber networks [1]. However, beyond optical transmission, multicore and few-mode fibers (FMFs) have also been applied to other fields, including, among others, sensing [2], astrophotonics [3], all-optical nonlinear processing [4], [5], [6], medical imaging [7], construction of high-power fiber lasers [8], and microwave photonics (MWP) [9], [10], [11], [12], [13], [14], [15], [16], [17], [18].

In MWP, the inherent parallelism of SDM fibers provides a compact platform to realize sampled true-time delay line (TTDL) operation, the basis of many radiofrequency (RF) signal processing functionalities [19]. TTDLs provide a series of time-delayed replicas of an input RF signal, where the adjacent samples have a constant basic differential time delay $\Delta\tau$ between them. By properly designing an SDM fiber, such that the different spatial paths (cores or modes) experience the adequate group delay, each path could provide one of the time-delayed

samples of the TTDL. This way, SDM technology not only distributes the signal but also processes it simultaneously, leading to "fiber-distributed signal processing" in a single optical fiber [9]. Moreover, SDM-based TTDLs offer two dimensional operation, since the sample diversity can be obtained in both space and optical wavelength. Along with the increased compactness, low weight and performance versatility provided by all SDM-based TTDLs, FMF-based solutions in particular offer an additional advantage, as their fabrication process is simpler and more cost-effective than that of multicore fibers.

To date, several theoretical and experimental FMF-based TTDL solutions, operating in the space diversity regime, have been reported [11], [12], [13], [14], [15], [16], [17], [18]. For example, in [13], [14], we experimentally demonstrated 3-sampled and 4-sampled TTDL operation over commercial FMFs, respectively, which required the inscription of long period gratings (LPGs) and could only operate at a single optical wavelength. Similarly, other reported experimental demonstrations of FMF-based TTDLs also fail to provide continuous tunability of the time delay with the optical wavelength [11], [12], [18], as they either only can work at a single wavelength or exhibit a wavelength-independent time delay. To address this issue, in [15], the inscription of 5 LPGs along a ring-core FMF was theoretically proposed to adjust the group delay of the FMF modes and provide 4-sampled TTDLs that are tunable with the optical wavelength; however, at the expense of increased complexity and performance instability. To overcome these limitations, we proposed a novel double-clad step-index FMF design in [17] (shown with dashed red lines in Fig. 1), where the dispersion properties of 5 of its modes were engineered such that they could theoretically provide a continuously tunable TTDL, without requiring any LPG inscriptions. Here, we have fabricated the said FMF and experimentally demonstrate, to the best of our knowledge, the first tunable FMF-based TTDL, in which the time delay can be continuously tuned over a wide range by simply changing the optical wavelength. Furthermore, the number of samples in this 5-sampled TTDL is higher than that of any of the previously reported FMF-based TTDLs operating in the space diversity regime.

II. CONTINUOUSLY TUNABLE FMF-BASED TTDL

For spatial mode n propagating in a FMF, the group delay τ_n at an optical wavelength λ can be expanded in a 1-st order Taylor series around an anchor wavelength λ_0, as:

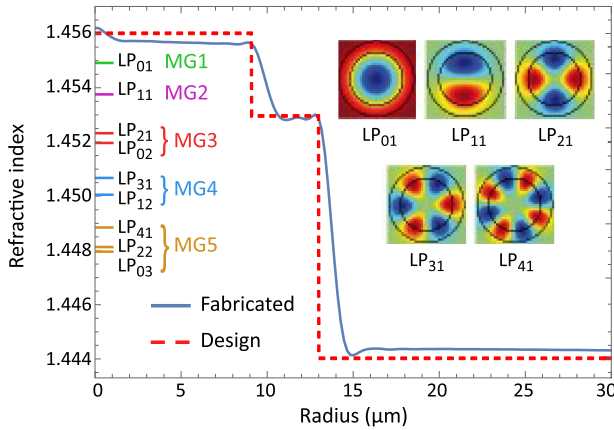$$\tau_n(\lambda) = [\tau_{0,n} + D_n(\lambda - \lambda_0)] L \qquad (1)$$

Fig. 1. Refractive index profile of the fabricated (solid blue) and designed (dashed red) [17] double-clad step-index FMF at 1550 nm. The horizontal colored lines depict the effective refractive indices of the supported modes in the first five mode-groups (MGs) of the fabricated FMF. In this FMF, tunable TTDL operation in the space diversity regime is possible for the 5 spatial modes shown on the right.

where $\tau_{0,n}$ and D_n denote the group delay per unit length and chromatic dispersion of mode n, at λ_0, respectively, while L is the fiber length. The implementation of a TTDL requires the basic differential group delay (DGD) between adjacent samples, $\Delta\tau$, to be constant. Depending on the operating regime (space or wavelength), the time-delayed samples are constructed differently in the FMF and therefore $\Delta\tau$ is defined differently [17].

In the space diversity, the time-delayed samples at a given wavelength are provided by the spatial modes propagating in the FMF and a constant $\Delta\tau(\lambda) = \tau_{n+1}(\lambda) - \tau_n(\lambda)$ between all adjacent samples requires the dispersion characteristics of the FMF modes to be properly engineered. Furthermore, for continuous tunability of the time-delay within an optical wavelength range, $\Delta\tau$ should have a linear behavior with the optical wavelength and the differential chromatic dispersion $\Delta D = D_{n+1} - D_n$ between adjacent modes should be constant at the anchor wavelength [17]. Given that in general, the modes within one mode-group feature similar dispersion properties, they are not suitable for being used as different TTDL samples. Therefore, for providing the time-delayed samples, modes from different mode-groups are considered. Accordingly, in this work, when referring to adjacent modes, we refer to the modes within adjacent mode-groups that satisfy the necessary requirements of a tunable TTDL.

In the wavelength diversity, a given mode is fed by several laser sources operating at different optical wavelengths and the time-delayed samples are provided by the different group velocities of the wavelengths propagating through that mode. Therefore, for mode n, we have $\Delta\tau_n(\lambda_m, \lambda_{m+1}) = \tau_n(\lambda_{m+1}) - \tau_n(\lambda_m)$, which indicates that by appropriately choosing the spacing between the wavelengths of the laser sources, a constant $\Delta\tau$ and consequently TTDL operation can be obtained.

Taking the aforementioned TTDL requirements into account, in a previous work [17], we designed a novel double-clad step-index FMF for the realization of a continuously tunable FMF-based TTDL. The doping amount and the radius of the core, inner

and outer cladding were designed using COMSOL together with an optimization process, such that the relative standard deviation (RSD) of ΔD was minimized at 1550 nm. The RSD is defined as:

$$\text{RSD} = \frac{\sigma_{\Delta D}}{\overline{\Delta D}}, \qquad (2)$$

where $\sigma_{\Delta D}$ and $\overline{\Delta D}$ represent the standard deviation and the average differential chromatic dispersion among adjacent modes, respectively. Through simulations, we showed that 5 spatial modes of the deigned FMF, namely LP_{01}, LP_{11}, LP_{21}, LP_{31} and LP_{41}, which belong to 5 different mode-groups, feature evenly-spaced incremental modal chromatic dispersion values (constant ΔD), making them suitable for tunable TTDL operation. Hereafter, we will refer to these 5 modes as the modes of interest. To verify our simulations experimentally, the designed FMF was recently fabricated by YOFC company. The refractive index profile of the fabricated (solid bule) and designed (dashed red) 1-km long FMF at 1550 nm, are shown in Fig. 1. The discrepancy observed between their refractive index profiles, which is due to fabrication imperfections, affects the dispersion properties of the modes. However, such variations in the geometry and doping amount of the core and claddings are within the tolerance range of the designed FMF-based TTDL. The GeO_2 doping concentration of the fabricated core, inner and outer cladding are around 7.79 mol%, 5.93 mol% and 0.22 mol%, while their radii are 9.1, 13 and 62.5 μm, respectively. The effective refractive indices of the supported modes in the first 5 mode-groups of the fabricated FMF, at 1550 nm, are shown in Fig. 1. Among them, in this work, we have only considered the 5 modes of interest since the dispersion properties of the other modes do not satisfy the required conditions for TTDL operation.

III. CHARACTERIZATION OF THE FABRICATED FMF

We used the setup of Fig. 2 to first characterize the fabricated FMF and then use it as a TTDL and measure its corresponding RF filtering response, while exploiting the space and wavelength diversities. In the spatial diversity domain, the optical signal coming from a broadband source (to avoid optical interference between the fiber modes) followed by a 0.1-nm-bandwidth optical filter is amplified by an erbium-doped fiber amplifier (EDFA) and employed as the input signal. Meanwhile, in the wavelength diversity domain, a set of lasers operating at evenly-spaced optical wavelengths are used as the input signal. In both diversities, the input signal is then intensity modulated by an RF signal generated by a vector network analyser (VNA). The frequency of the RF signal is swept from 10 MHz to 40 GHz and its power is 5 dBm. After amplification, the modulated signal is split into 5 paths (corresponding to the 5 modes of interest), the polarization of each path is controlled and the signal is injected/extracted into/from the desired mode (or modes) using a mode multiplexer/demultiplexer fabricated by Cailabs. The average insertion loss and the average modal crosstalk for the mode multiplexer and demultiplexer pair, measured in back-to-back measurements when they are spliced together, are 10.5 dB and -17.9 dB at 1530 nm, and 9.3 dB and -19 dB at 1565 nm, respectively. For each of the asymmetrical LP_{lm} modes ($l \geq 1$),
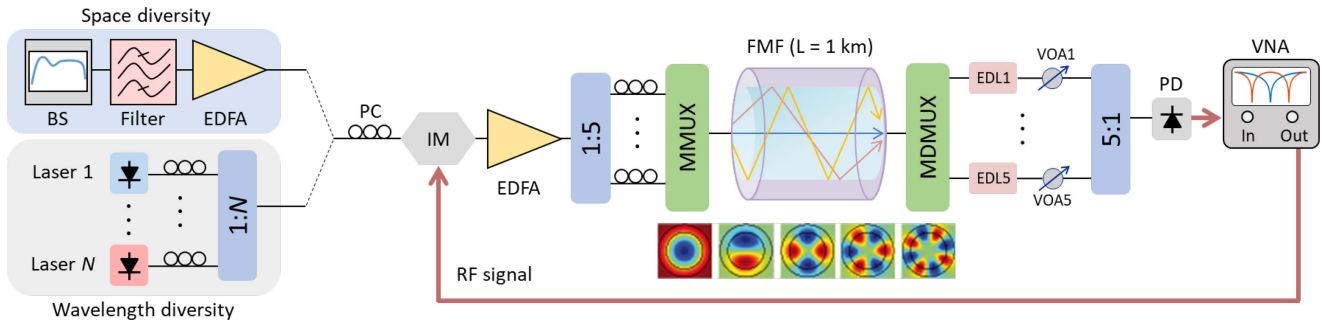
Fig. 2. Experimental setup used for the FMF characterization and also the measurement of the corresponding RF filter transfer functions when exploiting the space and wavelength diversities. BS: broadband source, EDFA: erbium-doped fiber amplifier, PC: polarization controller, IM: intensity modulator, MMUX: mode multiplexer, MDMUX: mode demultiplexer, EDL: external delay line, VOA: variable optical attenuator, PD: photodetector, VNA: vector network analyser.

only one of its two degenerate modes is demultiplexed; therefore, the power in that particular degenerate mode is maximized by adjusting the polarization controllers placed at the input of the multiplexer. To minimize coupling among the modes, we kept the FMF spool untouched and as stable as possible to reduce the effect of external coupling sources, such as bending, twisting and pressure applied to the fiber. Nevertheless, even though coupling between degenerate modes affects the output power in each of those modes, it has a negligible effect on $\Delta\tau$, since the group velocity associated with both degenerate modes is very similar.

Once the modes are demultiplexed at the output of the 1-km FMF, depending on the operation regime, the signals are handled differently. In the wavelength diversity regime, a single mode is detected, while in the space diversity regime, first, short lengths of single-mode fibers (SMFs), which we will refer to as external delay lines (EDLs), and variable optical attenuators (VOAs) are introduced into the optical path of each mode and then all modes are combined and detected jointly. The lengths of the SMFs employed as EDLs are chosen such that at the desired anchor wavelength (in our case $\lambda_0 = 1503$ nm), identical $\tau_{0,n}$ values are obtained for the 5 modes; in other words, the DGD among the modes are compensated at this wavelength and hence $\Delta\tau = 0$ is achieved (see (1)). The SMF lengths used for modes $\{LP_{01}, LP_{11}, LP_{21}, LP_{31}, LP_{41}\}$ are $\{1.82, 1.42, 0.72, 0.28, 0\}$ m, respectively, which are much shorter than the 1-km long FMF and therefore the effect of these EDLs on the overall chromatic dispersion behavior of the fiber link is negligible. Once the DGD is compensated at the anchor wavelength, no further EDL adjustments are required for operating at different wavelengths. This is due to the particular design and dispersion-diversity behavior of the FMF, which provides the desired time-delay tunability at wavelengths longer than the anchor wavelength. The VOAs are used to equalize the powers of different paths and obtain uniform amplitude distribution. The different power levels among different paths are due to the mode-dependent losses of the multiplexer/demultiplexer pair, the mode-dependent propagation losses in the FMF link and the coupling between degenerate modes.

Using the space diversity domain of Fig. 2, a microwave interferometric technique [20] was employed to measure the DGD between the 5 modes of interest at different optical wavelengths. This technique takes advantage of the fact that the RF signals modulated on the modes interfere with each other in the photodetector, and uses the resulting interference pattern, measured by the VNA, to extract the DGDs among the different modes. The measured DGDs of the modes with respect to LP_{01}, over a range of 1530 to 1565 nm, are displayed in Fig. 3(a). From these measurements, the average $\Delta\tau$ at each wavelength (green squares) and its corresponding standard deviation (error bars) are calculated and shown in Fig. 3(b). As observed, the average $\Delta\tau$ shows a linear behavior with the optical wavelength, confirming that the fabricated FMF can operate as a continuously tunable TTDL. By sweeping the wavelength over the 35-nm range of the C-band, the time delay can be continuously tuned from 46.3 to 105.6 ps. The error bars indicate that at every wavelength, the $\Delta\tau$ values among adjacent modes are not identical and have slight mismatches, but these small amounts of error are acceptable as the FMF-based TTDL can still provide microwave filters with adequate responses, as will be shown in the next section. According to the measured $\Delta\tau$ values, the corresponding free spectral range (FSR $= 1/\Delta\tau$) of an RF filter realized based on this TTDL, operating in the space diversity regime, is calculated and displayed in red in Fig. 3(b), which shows that the FSR can be reconfigured from 21.6 down to 9.5 GHz by changing the optical wavelength over the C-band.

To measure the modal chromatic dispersion, we first measured the group delay $\tau(\lambda)$ of each spatial mode at different wavelengths and then calculated the dispersion through $D = d\tau/d\lambda$. Note that from the measured differential group delay values of Fig. 3(a), we can extract the differential dispersion ΔD among the modes, but not the dispersion values themselves. We used a microwave interferometric technique, similar to the one used in the aforementioned space diversity DGD measurements, to measure the group delay of each mode; however, this time the measurements were carried out by exploiting the wavelength diversity domain of Fig. 2, where different wavelengths, ranging from 1530 to 1565 nm in 5-nm steps, were injected into a single mode. After detecting the power in that particular mode, the interference response is measured and the modal group delays relative to 1530 nm are extracted. The dispersion of each mode is then evaluated by taking the derivative of the group delays with
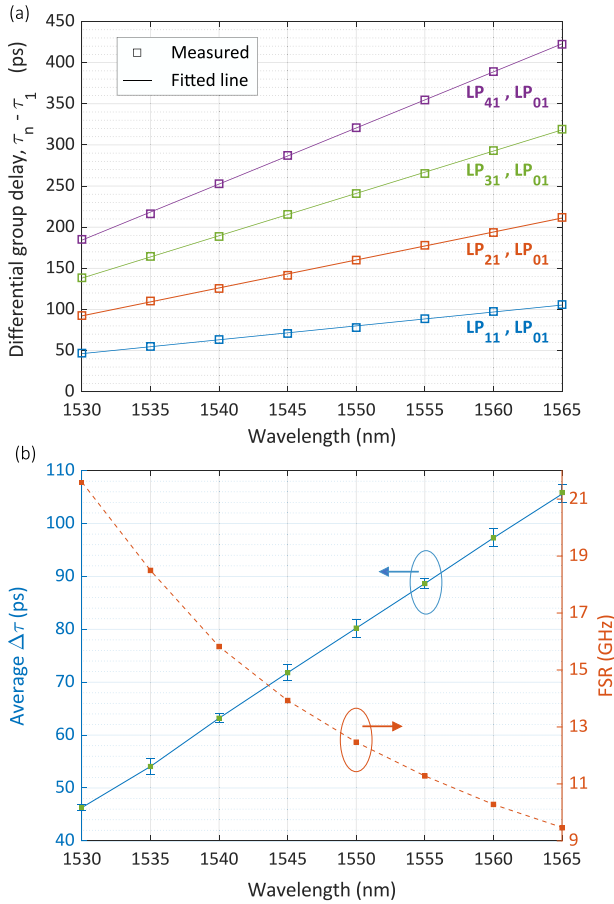
Fig. 3. (a) Measured (squares) and fitted (solid line) differential group delays of the modes of interest with respect to the fundamental LP_{01} mode. (b) Left axis: the mean $\Delta\tau$ values (green squares) and their corresponding error bars (in blue) at different wavelengths. Right axis: the corresponding free spectral range of a microwave filter implemented using the FMF-based TTDL operating in the space diversity regime (in red).
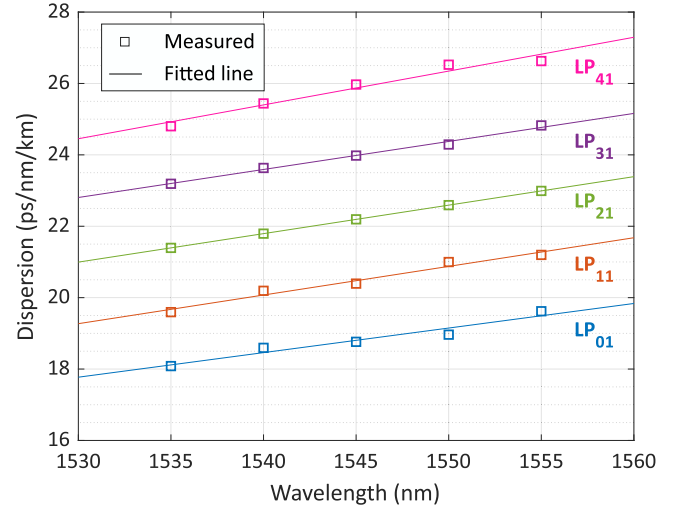

Fig. 4. Measured (squares) and fitted (solid lines) chromatic dispersion of the modes of interest, extracted from the group delay values measured in the wavelength diversity domain.

respect to the wavelength. The results, shown in Fig. 4, show that the modal dispersion increases with the mode order in relatively constant steps ($\Delta D \approx 1.7$ ps/nm/km at 1535 nm), satisfying the required condition for TTDL operation. The evaluated ΔD values are in agreement with those found from Fig. 3(a).

It should be noted that if for a particular application, $\Delta\tau$ values different from those obtained here are required, one can simply reconfigure the setup by moving the anchor wavelength to a value different from $\lambda_0 = 1503$ nm, through proper adjustment of the EDLs. This will change the DGD and consequently the average $\Delta\tau$ among the modes at each wavelength. Moreover, since the chromatic dispersion increases in relatively constant steps among adjacent modes, even if the anchor wavelength changes, the average $\Delta\tau$ will still maintain its linear behavior with the optical wavelength.

IV. EXPERIMENTAL DEMONSTRATION OF RF SIGNAL FILTERING

The performance of the fabricated TTDL was evaluated by applying it to RF signal filtering in two scenarios, one exploiting the space diversity and the other, the wavelength diversity, using the corresponding setup to each diversity, as shown in Fig. 2.

In the space diversity regime, we used the samples from the 5 modes of interest (LP_{01}, LP_{11}, LP_{21}, LP_{31} and LP_{41}) to construct 5-tap filters at different wavelengths. Figs. 5(a) and (b) depict the measured transfer functions of the realized RF filters. As expected, as the operating wavelength is swept over the C-band, from 1530 nm up to 1565 nm, reconfigurable microwave filters are obtained and the FSR of the filter is continuously tuned over a wide range, from 21.6 down to 9.5 GHz. This is in agreement with the results shown in Fig. 3(b) and confirms the tunability of our FMF-based TTDL.

In the wavelength diversity regime, two experiments were performed. First, the FMF modes, one at a time, were fed by an array of 7 lasers, whose wavelengths had 5-nm separations and ranged from 1530 to 1560 nm. Since the different modes have different dispersions, their $\Delta\tau$ values differ and consequently the FSR of the resulting 7-tap filters are different. This can be observed in Fig. 6(a), where as an example, the measured transfer functions of the RF filters implemented in three different modes are shown. For the sake of clarity, we have not included the responses corresponding to the other two modes (LP_{11} and LP_{31}). The FSR varies from 10.6 GHz for LP_{01} down to 7.7 GHz for LP_{41}. In another experiment, we injected an array of 10 lasers with wavelength separations of 2-nm, ranging from 1531 to 1549 nm, into each mode. The transfer function of the constructed 10-tap filters in different modes are shown in Fig. 6(b), where the FSR changes from 27.1 GHz for LP_{01} down to 19.8 GHz for LP_{41}. In this regime, as observed in Fig. 6, the FSR of the filter can be reconfigured by either changing the mode or the wavelength separation between the lasers. In practice, continuous tunability of the FSR in this regime would require several tunable lasers, which would make it more costly and complex than the space diversity regime, where only one wavelength tuning is required. Furthermore, the number of taps can be modified by varying the number of lasers as required.
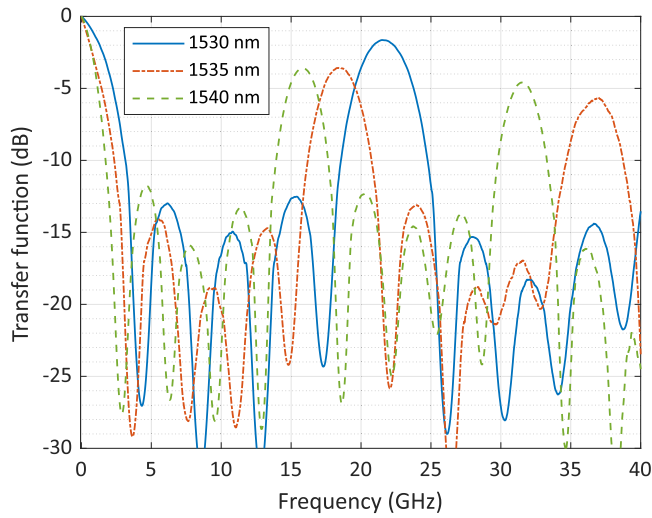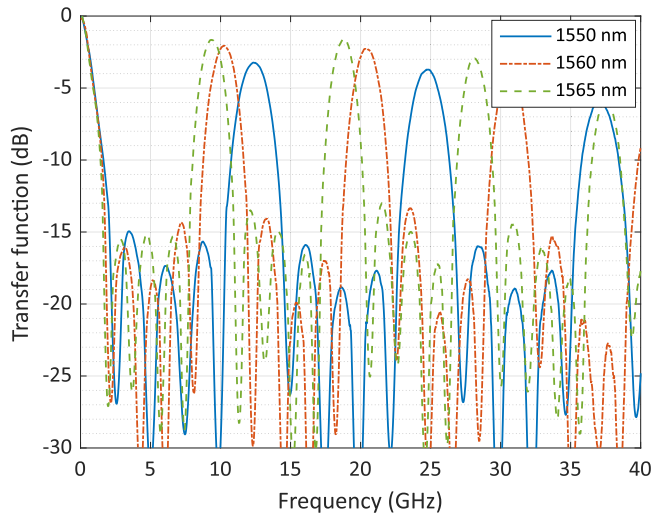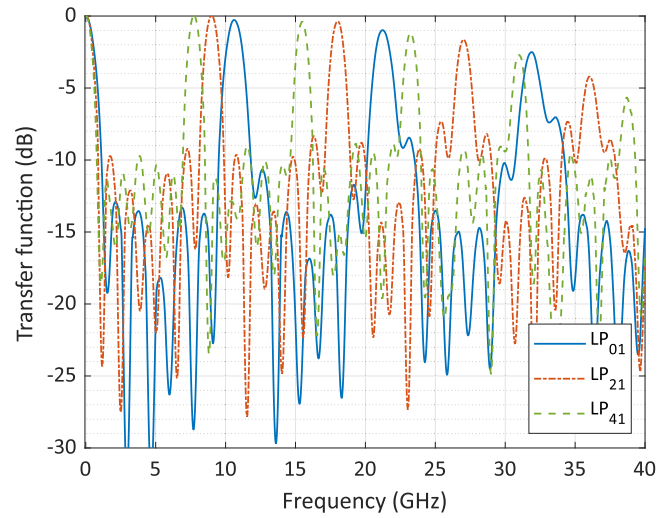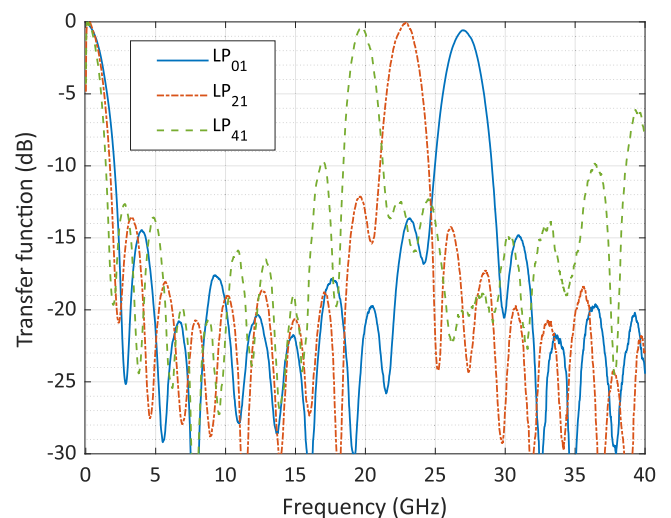
Fig. 5.   Measured RF signal filtering responses for TTDL operation in the space diversity domain, at different wavelengths within the optical C-band.

Fig. 6.   Measured RF signal filtering responses for TTDL operation in the wavelength diversity domain for 3 different modes, when a set of (a) 7 lasers with a 5-nm separation and (b) 10 lasers with a 2-nm separation, are used.

V. Conclusion

In the context of MWP signal processing, it is highly desirable to have reconfigurable RF signal processing, which in turn requires sampled TTDLs that can be continuously tuned over a wide range. The exploitation of FMFs to provide the required parallelization and group delay control for tunable sampled TTDL operation brings considerable advantages in terms of size, weight and power consumption reduction along with enhanced TTDL versatility. Here, to the best of our knowledge, we report the first experimental demonstration of a continuously tunable FMF-based TTDL. This has been enabled by the unique modal dispersion behavior of this dispersion-diversity FMF, i.e., the chromatic dispersion varies in relatively constant incremental steps (1.7 ps/nm/km at 1535 nm) among 5 different modes (LP_{01}, LP_{11}, LP_{21}, LP_{31} and LP_{41}), belonging to adjacent groups of modes. This delay line is applied to RF signal filtering, where reconfigurable 5-tap filters in the space diversity regime (with

FSRs ranging from 9.5 to 21.6 GHz) and 7 and 10-tap filters in the wavelength diversity regime (with FSRs ranging from 7.7 to 27.1 GHz), are realized, confirming that the FMF-based TTDL offers different delay line configurations within the same fiber link.

Beyond microwave signal filtering, this novel FMF can also enable a wide range of dispersion-managed optical signal processing applications, where the capability of providing incremental values of the chromatic dispersion, along with the exploitation of both the space and the optical wavelength dimensions, in a single optical fiber adds further flexibility and versatility. In the particular scenario of microwave photonics for 5G and Beyond communications, direct application is found in optical beamforming for phased-array antennas, arbitrary waveform generation and shaping, as well as multicavity optoelectronic oscillation, to cite a few.

REFERENCES

[1] D. J. Richardson, J. M. Fini, and L. E. Nelson, "Space-division multiplexing in optical fibres," *Nature Photon.*, vol. 7, no. 5, pp. 354–362, 2013.

[2] Y. Liu and L. Wei, "Low-cost high-sensitivity strain and temperature sensing using graded-index multimode fibers," *Appl. Opt.*, vol. 46, no. 13, pp. 2516–2519, May 2007.

[3] T. A. Birks et al., "Multicore optical fibres for astrophotonics," in *Proc. CLEO/Europe EQEC Conf. Dig.*, 2011, Paper JSIII2_1.

[4] E. Nazemosadat and A. Mafi, "Nonlinear switching in a two-concentric-core chalcogenide glass optical fiber for passively mode-locking a fiber laser," *Opt. Lett.*, vol. 39, no. 16, pp. 4675–4678, Aug. 2014.

[5] R. J. Essiambre et al., "Experimental investigation of inter-modal four-wave mixing in few-mode fibers," *IEEE Photon. Technol. Lett.*, vol. 25, no. 6, pp. 539–542, Mar. 2013.

[6] J. Gao et al., "Design, fabrication, and characterization of a highly nonlinear few-mode fiber," *Photon. Res.*, vol. 7, no. 11, pp. 1354–1362, 2019.

[7] Y. Choi et al., "Scanner-free and wide-field endoscopic imaging by using a single multimode optical fiber," *Phys. Rev. Lett.*, vol. 109, no. 20, Nov. 2012, Art. no. 203901.

[8] L. G. Wright, D. N. Christodoulides, and F. W. Wise, "Controllable spatiotemporal nonlinear effects in multimode fibres," *Nature Photon.*, vol. 9, no. 5, pp. 306–310, May 2015.

[9] I. Gasulla and J. Capmany, "Microwave photonics applications of multicore fibers," *IEEE Photon. J.*, vol. 4, no. 3, pp. 877–888, Jun. 2012.

[10] S. García, M. Ureña, and I. Gasulla, "Demonstration of distributed radiofrequency signal processing on heterogeneous multicore fibres," in *Proc. 45th Eur. Conf. Opt. Commun.*, Dublin, Ireland, 2019, pp. 1–4.

[11] K. H. Lee, W. Y. Choi, S. Choi, and K. Oh, "A novel tunable fiber-optic microwave filter using multimode DCF," *IEEE Photon. Technol. Lett.*, vol. 15, no. 7, pp. 969–971, Jul. 2003.

[12] D. V. Nickel, C. Villarruel, K. Koo, F. Bucholtz, and B. Haas, "Few mode fiber-based microwave photonic finite impulse response filters," *J. Lightw. Technol.*, vol. 35, no. 23, pp. 5230–5236, Dec. 2017.

[13] R. Guillem, S. García, J. Madrigal, D. Barrera, and I. Gasulla, "Few-mode fiber true time delay lines for distributed radiofrequency signal processing," *Opt. Exp.*, vol. 26, no. 20, pp. 25761–25768, Oct. 2018.

[14] S. García, R. Guillem, J. Madrigal, D. Barrera, S. Sales, and I. Gasulla, "Sampled true time delay line operation by inscription of long period gratings in few-mode fibers," *Opt. Exp.*, vol. 27, no. 16, pp. 22787–22793, 2019.

[15] S. García, R. Guillem, and I. Gasulla, "Ring-core few-mode fiber for tunable true time delay line operation," *Opt. Exp.*, vol. 27, no. 22, pp. 31773–31782, Oct. 2019.

[16] J. Zhao, H. Zhang, Z. Yang, J. Xu, T. Xu, and C. Wang, "Few-mode fibers with uniform differential mode group delay for microwave photonic signal processing," *IEEE Access*, vol. 8, pp. 135176–135183, 2020.

[17] E. Nazemosadat and I. Gasulla, "Dispersion-tailored few-mode fiber design for tunable microwave photonic signal processing," *Opt. Exp.*, vol. 28, no. 24, pp. 37015–37025, Nov. 2020.

[18] Y. Zhang, J. Gao, L. Zhu, S. Fu, Y. Wang, and Y. Qin, "Panda-type few-mode fiber-enabled microwave photonic filter with a reconfigurable finite impulse response," *Opt. Lett.*, vol. 46, no. 8, pp. 1852–1855, Apr. 2021.

[19] R. A. Minasian, "Photonic signal processing of microwave signals," *IEEE Trans. Microw. Theory Techn.*, vol. 54, no. 2, pp. 832–846, Feb. 2006.

[20] L. Wang, C. Jin, Y. Messaddeq, and S. LaRochelle, "Microwave interferometric technique for characterizing few mode fibers," *IEEE Photon. Technol. Lett.*, vol. 26, no. 17, pp. 1695–1698, Sep. 2014.

Elham Nazemosadat received the B.S. degree in electrical engineering from Shiraz University, Shiraz, Iran, in 2006, and the Ph.D. degree in electrical engineering from Nanyang Technological University, Singapore, in 2012. After working as a Postdoctoral Researcher with the University of Wisconsin-Milwaukee, Milwaukee, WI, USA, and Chalmers University of Technology Gothenburg, Sweden, she is currently with Universitat Politècnica de València, Valencia, Spain. Her research interests include applications of multicore and few-mode fibers in microwave photonics, design of specialty fibers, nonlinear Kerr effect in space-division multiplexed fibers for all-optical signal processing, silicon nitride waveguides, and microresonators.

Ivana Gasulla (Senior Member, IEEE) received the M.Sc. degree in telecommunications engineering and the Ph.D. degree in telecommunications from Universitat Politècnica de València (UPV), Valencia, Spain, in 2005 and 2008, respectively. She is currently an Associate Professor with UPV. From 2012 to 2014, she was a Fulbright Scholar with Stanford University, Stanford, CA, USA. Her research interests include the application of multimode and multicore fibers to microwave photonics systems. The results of her work have led to more than 125 international publications, highlighting contributions to nature communications and nature photonics. She was the recipient of the prestigious ERC Consolidator Grant to develop new Space-Division Multiplexing technologies for emergent fiber-wireless communications through the Project InnoSpace, in 2016. She is a Member of TPC of the most prestigious conferences in the field, such as the Optical Fiber Communication Conference and IEEE Photonics Conference. She is the Senior Editor of IEEE JOURNAL OF SELECTED TOPICS IN QUANTUM ELECTRONICS and an Associate Editor for IEEE PHOTONICS TECHNOLOGY LETTERS.